SAR reduction in deep brain stimulation patients using parallel transmission

Bastien Guerin[1], Sara Sprinkhuizen[1], Cristen LaPierre[1,2], Yigitcan Eryaman[1,3], and Lawrence L Wald[1,4]

[1]A. A. Martinos Center for Biomedical Imaging, Dpt. of Radiology, Massachusetts General Hospital, Charlestown, MA, United States, [2]Dpt. of Physics, Harvard University, Cambridge, MA, United States, [3]Madrid-MIT M+Vision Consortium in RLE, Massachusetts Institute of Technology, Cambridge, MA, United States, [4]Division of Health Sciences Technology, Harvard-MIT, Cambridge, MA, United States

Target audience: MR physicists, neuroscientists, neurosurgeons.

Purpose: Deep brain stimulation (DBS) leads are non-magnetic metallic brain implants used for the treatment of Parkinson disease, essential tremor and other conditions. Inside an MRI scanner, the RF transmit field induces strong currents on the lead, which penetrate brain tissues via electrodes thus creating a very large SAR hotspot. We show in simulations and phantom temperature measurements that parallel transmit (pTx) can dramatically reduce this effect by choosing excitation patterns where the tangential component of the electric field along the wire is minimal. The ability to safely study DBS patients with this method would yield crucial insight in the mechanisms of action of DBS, which are currently unknown.

Methods: Electromagnetic simulations: We simulated a patient with a DBS lead targeting the sub-thalamus nuclei (Fig. 1a) placed inside a 16 rungs high-pass head-only 3 T birdcage (BC) coil. We used a co-simulation strategy based on HFSS (Ansys, Canonsburg PA) [1,2]. This finite element electromagnetic field simulator allows modeling structures with widely different dimensions, which is crucial for simulation of a small DBS lead (1 mm diameter, Fig. 1c) placed inside a relatively large RF coil (37 cm diameter, Fig. 1b). We also simulated the same patient in an 8 channel pTx coil of similar dimensions (not shown). The BC coil was driven in 2 linear modes and a circularly polarized mode. For the pTx coil, magnitude least-squares RF shimming pulses were designed using an algorithm that constrained the 1 g local SAR at hundreds of location in the body, including at the tip of the lead, via virtual observation points (VOPs) [3,4]. Phantom temperature experiments: We 3D printed a head phantom containing a single compartment (whole head) filled with an ethylene glycol (EG) gel with 3% agar. The temperature dependence of the resonance frequency difference Δf between the hydroxyl and methylene group in EG is well known [5]. Acquisition of multi-echo GRE data (meGRE, 32 echoes with TEs ranging from 2 to 48 ms) provided an estimate of Δf, and hence the absolute temperature. We fit the meGRE signal in the time domain, which has been shown to be more robust than frequency analyses [6]. A copper wire with no insulation at its tip was placed in a quadrature 3 T BC coil (Siemens, Erlangen) which could be driven using either quadrature port independently (Fig. 2a). The temperature at the tip of the wire was monitored using a fluoroscopic thermometer with 0.1 ˚C accuracy (LumaSense, Santa Clara CA).

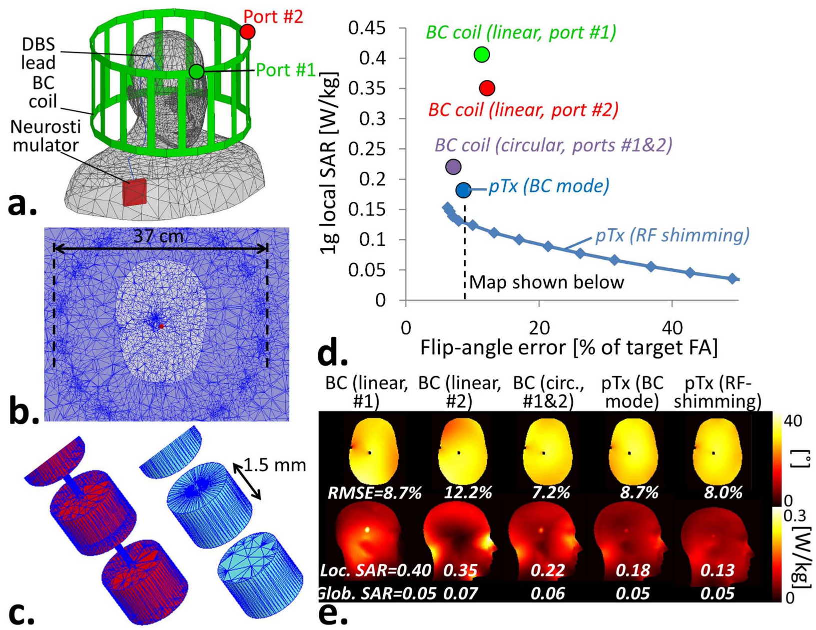

***Fig. 1. a**: HFSS simulation of a patient with a DBS lead targeting the sub-thalamus nuclei and imaged at 3 T using a birdcage (BC) coil. **b**: Transverse view of the HFSS tetrahedron mesh. **d**: Details of the mesh of the DBS lead (left: Conductive electrodes; right: Insulation). **d**: L-curves showing the tradeoff between the 1 g local SAR and the excitation error for the BC coil and an 8 channels pTx coil. **e**: Flip-angle (top) and SAR maximum intensity projection maps (bottom) for the BC coil and the 8 channel pTx coil.*

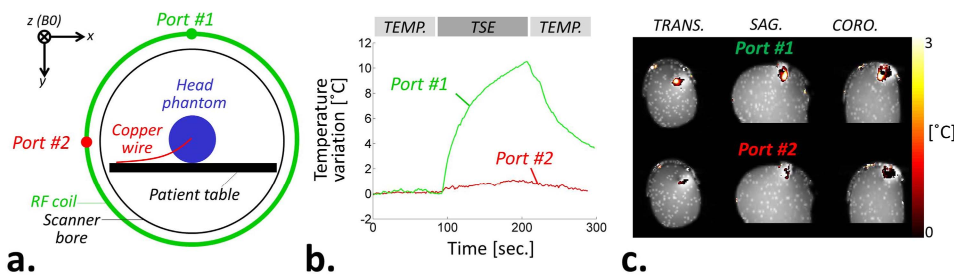

***Fig. 2. a**: Schematics of the experimental setup showing the head phantom filled with ethylene glycol gel and the two ports of the BC coil. A copper wire was placed in the head phantom and ran parallel to the bore in the z direction. **b**: Temperature variation at the tip of the wire (fluoroscopic thermometer). A TSE sequence was ran at high duty-cycle on either port #1 or port #2. Two multi-echo GRE sequences (TEMP.) were played before and after the TSE for temperature mapping. **c**: Difference temperature maps overlaid on the phantom anatomy showing a clear temperature increase at the tip of the wire when driving the BC coil with port #1.*

Results/Discussion: Fig. 1d shows that the pTx excitations achieved better tradeoffs between local SAR and flip angle uniformity than the local BC coil. Driving the BC coil using the port contained in the plane defined by the lead and its wire (port #2) also dramatically reduced SAR at the tip of the DBS lead compared to when using the other 90 degrees drive (port #1). However, this strategy increased SAR in the nose and the back of the head. Fig. 1e shows that pTx excitations reduced SAR everywhere including at the lead tip, in the nose and in the back of the head thanks to SAR optimization using the VOPs. In agreement with our simulations, in experiments with the BC coil we observed a dramatic temperature rise at the tip of the copper wire when using the port not contained in the plane defined by the wire (port #1, Fig. 2b). Use of the other quadrature port (port #2) created almost no temperature increase (this phenomenon was first observed by Eryaman et al. [7]). This is because the electric field of a linear BC coil has a null passing through the drive port. Placing the DBS lead in that null reduces coupling with the RF coil, which reduces the induced current on the lead wire and therefore SAR. Temperature mapping of the EG phantom before and after the heating sequence (high duty-cycle TSE) confirmed that the temperature increase was confined to a small region around the tip of the lead (Fig. 2c).

Aknowledgements: NIH R01EB006847, Siemens-MIT CKI Alliance, Comunidad de Madrid and the Madrid MIT M+Vision Consortium.

References: **[1]** Kozlov M. JMRI 2009;200(1):147-152. **[2]** Guérin B. ISMRM 2013 p2741. **[3]** Guérin B. MRM 2013. DOI: 10.1002/mrm.24800. **[4]** Eichfelder G. MRM 2011;66(5):1468-1476. **[5]** Amman. JMR 1982, 46:319-321. **[6]** Sprinkhuizen SM. MRM 2010;64(1):239-248. **[7]** Eryaman Y. MRM 2011;65(5):1305-1313.